Cellular Imaging

DOI: 10.1002/anie.201007297

Force-Induced Remnant Magnetization Spectroscopy for Specific Magnetic Imaging of Molecules**

*Li Yao and Shoujun Xu**

Molecular and cellular imaging often employs a labeling technique, which is usually optical labeling[1] or magnetic labeling,[2] to highlight target molecules and cells. While optical labeling uses a wavelength parameter to achieve molecular and cellular specificity, there is no analogous parameter in magnetic labeling, despite a variety of detection techniques having been developed.[3–7] This deficiency means that the magnetic field signal cannot be resolved into a group of individual signals based on molecular specificity. Consequently, no selectivity for target molecules has been achieved without sample separation. For example, the scanning magnetic imaging technique developed recently relies on a washing process to physically remove nonspecifically bound magnetic particles.[8] Alternatively, magnetic relaxation contrast measures the different relaxation times of free versus bound magnetic particles.[9] The associated shortcomings include a small difference in relaxation times and the lack of quantitatively resolving multiple relaxation processes.

Herein we present a technique that implements a spectroscopic character in magnetic detection for the identification of molecules and cells. This technique, force-induced remnant magnetization spectroscopy (FIRMS), uses an external force with varying amplitudes to induce dissociation of the bonds between the target molecules on cells and the ligand molecules conjugated on magnetic particles. At each force, the magnetization and spatial coordinates of the magnetic particles with the particular binding character are revealed by scanning magnetic imaging.

Figure 1 shows the experimental procedure. Cells that express specific receptors are incubated with magnetic particles. Particles conjugated with the corresponding ligands bind the receptor molecules, whereas particles with non-specific ligands are only physisorbed. The magnetic dipoles of all of the particles are initially aligned with an external magnetic field and, consequently, produce an overall magnetization (Figure 1 a). An external force is then applied to the cells incubated with magnetic particles. When the applied force exceeds the binding force of one group of magnetic particles (the physisorbed particles, for example), those particles will dissociate and undergo Brownian relaxation (Figure 1 b). The randomization of the magnetic dipoles of the dissociated particles makes no contribution to the measured magnetization;[10] therefore, the magnetization difference before and after the force disturbance represents the number of magnetic particles with this specific binding force to the target cells. By varying the force amplitude, a force spectrum is obtained. The spectrum reveals the quantities of all of the magnetic particles resolved with respect to their binding forces to the target molecules and cells. The magnetization and spatial information of the particles are measured using a scanning magnetic imaging technique (Figure 1 c).[11] Briefly, the sample containing magnetically labeled cells is scanned along the x axis across an atomic magnetometer. The resulting magnetic field profile provides the magnetization of the magnetic particles and spatial information (x, d) of the sample.

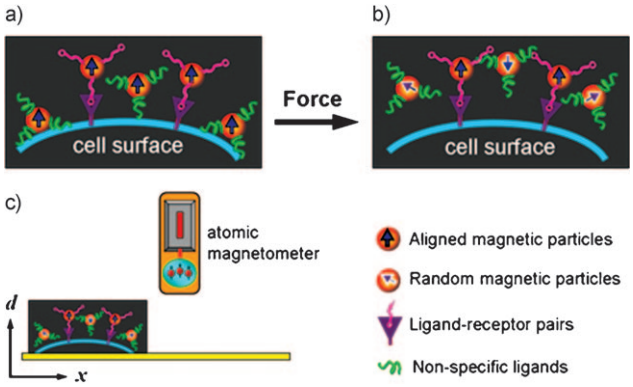

Figure 1. The FIRMS method. a) Binding between magnetic particles and cells without an external disturbing force; b) an external force induces dissociation of weakly-bound magnetic particles; c) scanning magnetic imaging. The sample is scanned along the x axis; the magnetic field along the d axis is measured by an atomic magnetometer during scanning.

Experimentally, we chose human CD3+ T cells binding to magnetic particles by the CD3 antibody. The CD3+ T cells play an important role in various diseases, such as diabetes[12] and HIV.[13] Figure 2 shows the magnetization as a function of force amplitude for three different binding conditions, with the force measured as the speed of a mixer that was used to exert force on the sample.

First a blank experiment was carried out in which there were no cells in the sample well, only magnetic particles and CD3 antibody (Figure 2, black trace). The disturbing force decreased the magnetization of the sample at around 1800 rpm (revolutions per minute) and entirely eliminated the magnetization at 2200 rpm. The disappearance of the magnetization indicated that all of the magnetic particles had

[*] Dr. L. Yao, Prof. S. Xu
Department of Chemistry, University of Houston
Houston, TX 77204 (USA)
Fax: (+1) 713-743-2709
E-mail: sxu7@uh.edu
Homepage: http://www.chem.uh.edu/Faculty/Xu/

[**] Support from the US National Science Foundation under grant ECCS-1028328 is acknowledged. This work is also supported in part by the Texas Center of Superconductivity at the University of Houston. We thank Prof. Chengzhi Cai for access to his laboratory resources.

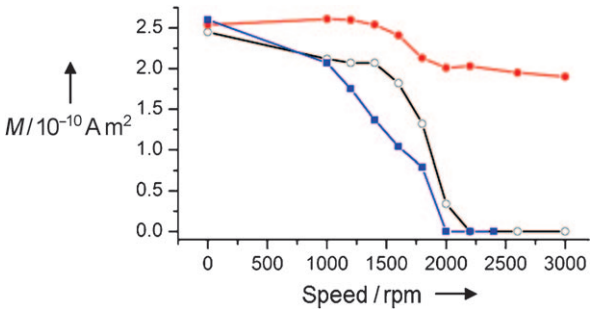

Figure 2. Magnetization as a function of the magnitude of an external force. ○, black curves: Blank experiment with only CD3 antibody and magnetic particles in the sample, and no cells present; ●, red: Cell-binding experiment, in which CD3+ T cells were incubated with CD3 antibody and magnetic particles; ■, blue: Control experiment, in which CD3+ T cells that were not conjugated with the CD3 antibody were incubated with magnetic particles.

undergone dissociation. In other words, no strongly bound particles were present in the absence of target cells.

The second experiment is the cell-binding experiment (Figure 2, red trace). Here, the sample contained target cells in addition to the same amounts of the magnetic particles and antibody as in the blank experiment. When there was no force, the magnetization was the same as in the blank because all the magnetic particles contributed to the signal. The gradually increasing force caused a similar decrease in magnetization but with much smaller amplitude. A strong signal remained even after a force of 3000 rpm was applied to induce dissociation. The magnetization change indicated that there were two types of binding for the magnetic particles, one binding similar to the blank and the other stronger binding. Clearly, the common features in the two experiments arise from physisorption between the magnetic particles and the surface of the sample well. The more strongly binding particles in the cell-binding experiment are due to the specific interaction between CD3-conjugated magnetic particles and CD3+ T cells.

The third experiment is the control experiment (Figure 2, blue trace). We incubated magnetic particles and cells without the CD3 antibody so that the magnetic particles were unable to specifically bind to the cells. The initial magnetic signal was close to those of the first two experiments, owing to the similar amount of magnetic particles. However, the signal decrease followed a different pattern from the previous two experiments. It first decreased at a faster pace than the blank and then dropped to zero near the same force as in the blank. The fact that the magnetization became zero in the absence of the antibody confirmed that the remaining magnetization in the previous experiment belonged to the particles specifically bound to the target cells.

These data show that without an external force, the magnetic signal gives no information regarding the binding behavior of the magnetic particles, as the signal is determined only by the overall quantity of the magnetic particles. However, when a variable force is applied, the change in magnetization provides patterns characteristic to the interaction between the magnetic particles and the target cells. The cells are static under our condition because their adhesive force is usually more than one order of magnitude stronger than the binding forces between antibody and antigen.[14]

To quantitatively elucidate the nature of the binding between the magnetic particles and the cells under various conditions, we took the derivatives of the magnetization curves. Because each magnetization change at a certain force represents the quantity of magnetic particles with that binding force, the resulting plots became a new type of spectra: force-induced remnant magnetization (FIRM) spectra (Figure 3a–c). The force was scaled to the physisorption peak in the blank experiment using Gaussian fitting. In the spectrum for the blank experiment (Figure 3a), the single peak was at 1.00, and the half-width at half-maximum was 0.11. This physisorption peak had 100% abundance because the magnetization became zero after this peak. The peak assignment with relative amplitudes is shown in Figure 3d. The spectrum for cell binding had a peak at a similar position (0.90) and width (0.11). The difference was that the peak height was only 30% of that in the blank spectrum, indicating that the remaining 70% of the magnetic particles were bound to the target cells by the characteristic CD3 binding pair (Figure 3e).

The spectrum for the control experiment had two peaks, one at 0.67 and the other at 1.00 (Figure 3c). The peak heights were 45% and 55% of the overall magnetization respectively. Because the latter peak was at the same position as the peak in the blank spectrum, we attributed it to the physisorption of the magnetic particles onto the sample well. Compared to the cell-binding experiment, the only difference in this control experiment was the introduction of a nonspecific cell surface. Therefore, the new peak at a weaker force was considered to be the nonspecific binding between the magnetic particles and the cell surface (Figure 3f). The slightly weaker force was possibly due to the smaller contact area between the particles

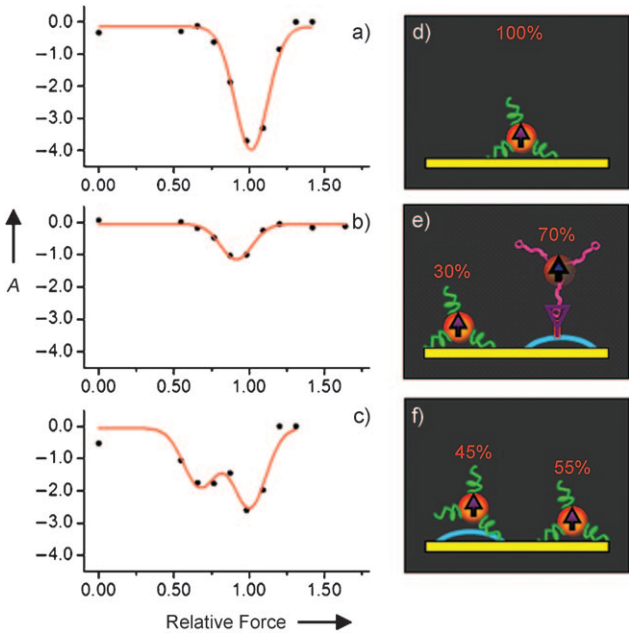

Figure 3. FIRM spectra and peak assignments (A = relative amplitude.) a)–c) FIRM spectra, showing the magnetization differential as a function of disturbing force for the blank, cell-binding, and control experiments. d)–f) Binding behaviors corresponding to the peaks shown in the FIRM spectra.

and the curved cells compared to the particles contacting the flat surface of the sample well.

Cellular uptake of magnetic particles has been studied by many other techniques.[15] Our results are consistent with these studies in that both cell-bound and unbound particles are observed. A unique feature of FIRMS is that it uses force to clearly resolve the specific cell-bound particles from the rest particles without requiring sample separation, which enables precise and rapid medical diagnostics.

The molecular specificity of FIRMS comes from the specific binding between antibody and its corresponding antigen, which is well studied.[16] As the strongly bound particles only appear when both antibody and its corresponding antigen are present, our technique is capable of identifying biological entities containing a specific antigen by using magnetic particles conjugated with appropriate antibody. Herein we showed CD3 antibody-conjugated magnetic particles could identify the presence of CD3+ T cells.

Combining FIRMS with scanning magnetic imaging, which provides the spatial information of magnetic signals in addition to magnetization,[8,11] we were able to obtain both the quantity and location of a specific group of magnetic particles. First, a magnetization of 2.5×10^{-10} A m^2 at a force of zero corresponds to 2 μg of particles, which contains 2.0×10^5 particles. Given the percentages in the cell-binding experiment, we determined that 1.4×10^5 particles were bound to the cells by the CD3 antibody and 6×10^4 particles were physisorbed by the sample well. In the control experiment, 9×10^4 particles were physisorbed by the cells, and 1.1×10^5 particles were physisorbed by the sample well. Second, resolving magnetic particles by their binding forces will lead to more accurate spatial information for the target cells, because magnetic particles that are not specifically bound to target cells will no longer interfere with the signal. The spatial coordinates for the cell-bound particles, hence the cells, are $x=(244\pm0.2)$ mm and $d=(8.9\pm0.03)$ mm in the cell-binding experiment.

In conclusion, the FIRMS technique was developed to resolve magnetic particles based on their binding forces. Its application in the imaging of human T cells quantitatively revealed several different binding types, which has not been achieved with existing techniques. Future work includes calibrating the binding forces[17] and improving detection sensitivity to provide more detailed information for magnetic molecular and cellular imaging.[18]

Experimental Section

In the cell-binding experiment, a suspension of human CD3+ T cells (500 μL, ca. 1×10^7 cells, Innovative Research) was incubated with biotinylated human CD3 antibody (25 μL, Invitrogen) for 10 min at 2–8 °C. The cells were then washed with phosphate-buffered saline (PBS; 2 mL), centrifuged for 8 min, and re-suspended in PBS (50 μL). All PBS buffers contained 0.1% bovine serum albumin (BSA) and 2 mM ethylenediaminetetraacetic acid (EDTA). Magnetic dynabeads with a streptavidin coating (Invitrogen) were used to capture the T cells. 2 μL of the cell suspension (ca. 4×10^5 cells) with the CD3 antibody and 2 μL of magnetic particle solution (1 mg mL^{-1}) were added to a sample well of $4\times1\times1$ mm^3. The sample well was covered with glass, and the sample was incubated for 8 h. A vortex mixer (VWR, 945303) was used to apply forces to the sample cell for 5 min. Magnetization measurements were performed using scanning magnetic imaging with an atomic magnetometer with a sensitivity of about 200 fT Hz$^{-1/2}$.

Received: November 19, 2010
Revised: January 31, 2011
Published online: April 11, 2011

Keywords: atomic magnetometry · cellular imaging · magnetic nanoparticles · molecular specificity · scanning force microscopy

[1] a) R. Y. Tsien, *Annu. Rev. Biochem.* **1998**, *67*, 509–544; b) W. Min, S. Liu, S. Chong, R. Roy, G. R. Holtom, S. Xie, *Nature* **2009**, *461*, 1105–1109.
[2] a) J.-M. Nam, C. S. Thaxton, C. A. Mirkin, *Science* **2003**, *301*, 1884–1886; b) S. Laurent, D. Forge, M. Port, A. Roch, C. Robic, L. V. Elst, R. N. Muller, *Chem. Rev.* **2008**, *108*, 2064–2110.
[3] a) D. Budker, V. V. Yashchuk, R. Zolotorev, *Phys. Rev. Lett.* **1998**, *81*, 5788–5791; b) I. K. Kominis, T. W. Kornack, J. C. Allred, M. V. Romalis, *Nature* **2003**, *422*, 596–599.
[4] M. Pannetier, C. Fermon, G. Le Goff, J. Simola, E. Kerr, *Science* **2004**, *304*, 1648–1650.
[5] Y. R. Chemla, H. L. Grossman, Y. Poon, R. McDermott, R. Stevens, M. D. Alper, J. Clarke, *Proc. Natl. Acad. Sci. USA* **2000**, *97*, 14268–14272.
[6] B. Gleich, J. Weizenecker, *Nature* **2005**, *435*, 1214–1217.
[7] a) J. R. Maze, P. L. Stanwix, J. S. Hodges, S. Hong, J. M. Taylor, P. Cappellaro, L. Jiang, M. V. G. Dutt, E. Togan, A. S. Zibrov, A. Yacoby, R. L. Walsworth, M. D. Lukin, *Nature* **2008**, *455*, 644–647; b) G. Balasubramanian, I. Y. Chan, R. Kolesov, M. Al-Hmoud, J. Tisler, C. Shin, C. Kim, A. Wojcik, P. R. Hemmer, A. Krueger, T. Hanke, A. Leitenstorfer, R. Bratschitsch, F. Jelezko, J. Wrachtrup, *Nature* **2008**, *455*, 648–651.
[8] L. Yao, A. C. Jamison, S.-J. Xu, *Angew. Chem.* **2010**, *122*, 7655–7658; *Angew. Chem. Int. Ed.* **2010**, *49*, 7493–7496.
[9] H. L. Grossman, W. R. Myers, V. J. Vreeland, R. Bruehl, M. D. Alper, C. R. Bertozzi, J. Clarke, *Proc. Natl. Acad. Sci. USA* **2004**, *101*, 129–134.
[10] R. Kötitz, H. Matz, L. Trahms, H. Koch, W. Weitschies, T. Rheinländer, W. Semmler, T. Bunte, *IEEE Trans. Appl. Superconduct.* **1997**, *7*, 3678–3681.
[11] L. Yao, S.-J. Xu, *Angew. Chem.* **2009**, *121*, 5789–5792; *Angew. Chem. Int. Ed.* **2009**, *48*, 5679–5682.
[12] A. Kaufman, K. C. Herold, *Diabetes Metab. Res. Rev.* **2009**, *25*, 302–306.
[13] J. L. Foster, J. V. Garcia, *Retrovirology* **2008**, *5*, 84.
[14] a) G. Guillemot, S. Lorthois, P. Schmitz, M. Mercier-Bonin, *Chem. Eng. Res. Des.* **2007**, *85*, 800–807; b) J. W. Weisel, H. Shuman, R. I. Litvinov, *Curr. Opin. Struct. Biol.* **2003**, *13*, 227–235.
[15] a) H. Zhang, P. S. Williams, M. Zborowski, J. J. Chalmers, *Biotechnol. Bioeng.* **2006**, *95*, 812–829; b) K. Peldschus, A. Schultze, P. Nollau, M. Kaul, U. Schumacher, C. Wagener, G. Adam, H. Ittrich, *Magn. Reson. Imaging* **2010**, *28*, 599–606; c) S.-H. Song, H.-L. Lee, Y. H. Min, H.-I. Jung, *Sens. Actuators B* **2009**, *141*, 210–216.
[16] a) J. D. Adams, U. Kim, H. T. Soh, *Proc. Natl. Acad. Sci. USA* **2008**, *105*, 18165–18170; b) M. Takahashi, T. Yoshino, H. Takeyama, T. Matsunaga, *Biotechnol. Prog.* **2009**, *25*, 219–226.
[17] a) V. T. Moy, E. L. Florin, H. E. Gaub, *Science* **1994**, *266*, 257–259; b) R. Merkel, P. Nassoy, A. Leung, K. Ritchie, E. Evans, *Nature* **1999**, *397*, 50–53.
[18] H. B. Dang, A. C. Maloof, M. V. Romalis, *Appl. Phys. Lett.* **2010**, *97*, 151110.

